

Selective Synthesis of Dimethylamine over Small-Pore Zeolites

III. H-ZK-5

R. D. SHANNON, M. KEANE, JR., L. ABRAMS, R. H. STALEY, T. E. GIER,
AND G. C. SONNICHSEN

*E. I. du Pont de Nemours & Company,¹ Central Research and Development Department,
Experimental Station, Wilmington, Delaware 19880*

Received August 25, 1987; revised July 27, 1988

H-ZK-5 is a highly selective catalyst for dimethylamine (DMA) synthesis in the reaction of methanol and ammonia. Deep-bed (DB) calcination of NH_4 -ZK-5 containing 4 Cs/uc results in DMA selectivities of 60-75% but with 15-30% dimethyl ether (DME) yields. Deep-bed or shallow-bed steam calcination of NH_4 -ZK-5 with only 1 Cs/uc gives similar high DMA selectivities but lower DME yields of 5-10%. Shallow-bed calcination of NH_4 -ZK-5 results in DMA selectivities of ~45%. The activity of H-ZK-5 in the methylamine synthesis reaction is lower than that of zeolite H-RHO. © 1989 Academic Press, Inc.

INTRODUCTION

Zeolite H-ZK-5 is a highly selective and active catalyst for dimethylamine synthesis from the reaction of methanol and ammonia (1-3). As with zeolite H-RHO described in Parts I and II of this series (4, 5), the dimethylamine (DMA) and trimethylamine (TMA) selectivities of H-ZK-5 depend on calcination conditions. This paper describes the physical and catalytic properties of ZK-5 catalysts prepared by deep-bed and shallow-bed calcination techniques.

EXPERIMENTAL

Zeolite Preparation and Characterization

K,Cs-ZK-5 was prepared according to the procedure of Robson (6, Example 3). Three different batches of ZK-5 (A, B, and C) were evaluated. All were synthesized from a $\text{K}_2\text{O}-\text{Cs}_2\text{O}-\text{Al}_2\text{O}_3-\text{SiO}_2$ gel using Ludox HS-40 and Alcoa C-37 $\text{Al}(\text{OH})_3$. Scanning electron micrographs showed the presence of cubic crystallites (0.2-1.0 μm) with rounded edges. One preparation (C)

contained debris in the form of small spheres and perhaps gel.

NH_4 -ZK-5 was prepared by 3, 8, or 12 exchanges for 4 h in 10% aq NH_4NO_3 at 80°C using a solid:liquid ratio of 1:10 by weight. Cs removal from Cs,K-ZK-5 is more difficult than that from Cs,Na-RHO. It takes 3 NH_4^+ exchanges of Cs,Na-RHO to get to 3.6% Cs (0.87 Cs/uc) whereas it takes 3 exchanges of Cs,K-ZK-5 to get to 7.5% Cs (3.9 Cs/uc), 8 exchanges to get to 3.8% Cs (2.1 Cs/uc), and 12 exchanges to get to 2.1% Cs (1.1 Cs/uc).

Four calcination procedures were used: dry shallow-bed (SBN), shallow-bed steaming (SBST), deep-bed (DB), and stagnant deep-bed (SDB). Shallow-bed calcination consisted of moving a 5- to 10-g sample, in a quartz boat of 100 cm^2 area, through the hot zone of a belt furnace for 4 h. Rapid removal of H_2O and NH_3 was assured by a 20 liter/min flow of N_2 over the sample. Steamed H-ZK-5 was prepared by heating NH_4 -ZK-5 for 1 h under 1 liter/min N_2 to produce H-ZK-5 and then maintaining the sample at temperature for 4 h under 1 liter/min N_2 having the desired H_2O content. Deep-bed calcination was carried out

¹ Contribution No. 4500.

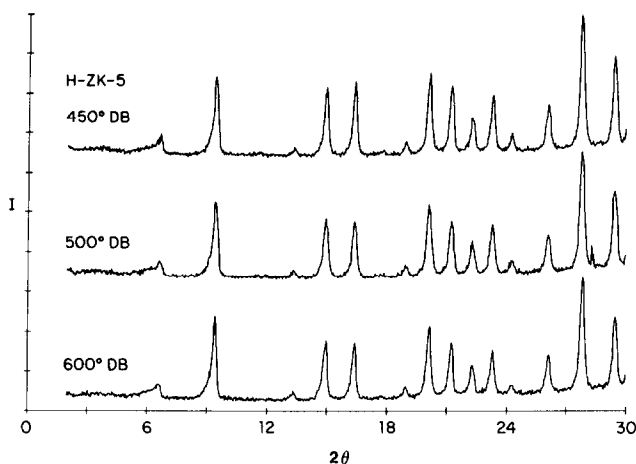


FIG. 1. X-ray diffraction patterns of H-ZK-5 deep-bed calcined at 450, 500, and 600°C.

for 10 h at 450–600°C using a 5-g sample placed in a covered crucible of 2.5 cm in diameter and 5.0 cm in height. Stagnant deep-bed calcination was carried out for 17 h at 500 or 650°C according to the procedure described earlier (7, 8). Samples of $\text{NH}_4\text{-ZK-5}$ were slowly heated to 500 or 650°C in air in a quartz tube attached to a glass manifold. The manifold was vented to the atmosphere through a partially open stopcock to avoid pressure buildup on heating. Other than a slight displacement of air caused by heating, there was no other gas flow. Water condensation in the tubing

above the sample was observed throughout the calcination treatment. Because the manifold line was at room temperature, the resulting partial pressure of water within the manifold was estimated to be 20 Torr.

X-ray diffraction patterns were obtained on a Philips APD 3600 diffractometer using $\text{CuK}\alpha$ radiation. Typical patterns for DB, SBN, SBST, and SDB samples are shown in Figs. 1–4. Infrared experiments were performed according to the procedure previously described (8, 9). Internal Lewis site concentration was estimated from adsorption of MeCN. Methanol sorption measure-

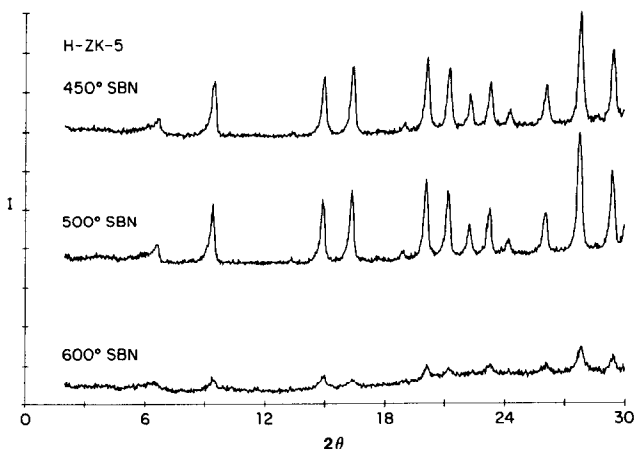


FIG. 2. X-ray diffraction patterns of H-ZK-5 shallow-bed calcined at 450, 500, and 600°C.

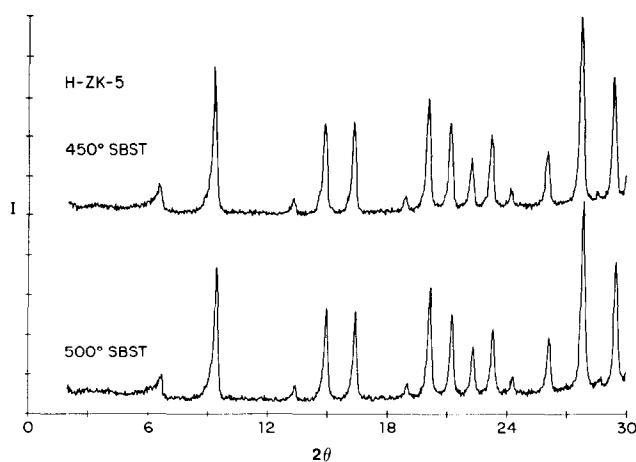
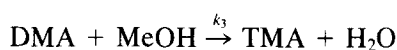
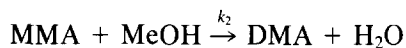
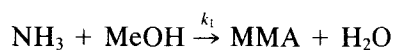


FIG. 3. X-ray diffraction patterns of H-ZK-5 steam calcined at 450 and 500°C.

ments, described earlier (8), were used to study framework damage. The ratio of methanol to *n*-propanol sorption after 20 h of exposure, defined as a geometric selectivity index (GSI), was used as a measure of pore constriction (2).

The catalytic behavior of the samples was evaluated in a U-tube reactor at temperatures of 250–400°C using a methanol: ammonia mixture at a molar ratio of 1:1. Details are given in Ref. (4). The data were fit to a second-order reaction mechanism described in Keane *et al.* (1) which includes

three primary series-parallel reactions, using the scheme



The primary relative rate constants of interest are DMA formation relative to TMA formation, k_2/k_3 and TMA formation, k_3 , where k_1 is set to 1. Values of $k_2/k_3 > 1$

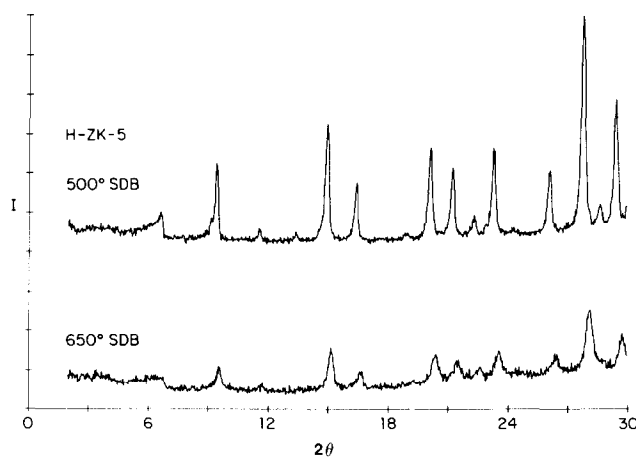


FIG. 4. X-ray diffraction patterns of H-ZK-5 stagnant deep-bed calcined at 500 and 650°C.

TABLE I
 Characterization H-ZK-5

| Sample | T_c | h | Cs/uc | $\nu(T-O)$ | Sorption g/100 g | | T | Conv (%) | DME (%) | DMA (%) | TMA (%) | GSI | SV (h^{-1}) | k_2 | k_3 | k_2/k_3 |
|--|-------|-----|-------|------------|------------------|------------------------|-----|----------|---------|---------|---------|-----|-----------------|-------|-------|-----------|
| | | | | | MeOH 20 h | <i>n</i> -PrOH 20 h | | | | | | | | | | |
| A. Deep-bed calcination (DB) | | | | | | | | | | | | | | | | |
| A | 450 | 10 | 4.0 | 1077 | 20.4 | 16.3 | 325 | 98 | 15 | 45 | 30 | 1.2 | 1.2 | 4.7 | 1.3 | 3.5 |
| A | 500 | 10 | 4.0 | 1075 | 19.9 | 12.8 | 325 | 94 | 25 | 52 | 21 | 1.5 | 1.1 | 5.8 | 1.3 | 4.4 |
| A | 600 | 10 | 4.0 | 1076 | 18.6 | 5.2 | 325 | 98 | 30 | 72 | 6 | 3.6 | 0.8 | 4.3 | 0.4 | 10.4 |
| B | 450 | 10 | 1.1 | 1071 | 21.5 | 3.7 | 350 | 92 | 11 | 65 | 13 | 5.8 | 1.2 | 5.6 | 0.8 | 6.9 |
| B | 500 | 10 | 1.1 | 1074 | 20.9 | 4.4 | 350 | 92 | 4 | 65 | 12 | 4.7 | 0.7 | 4.9 | 0.6 | 8.0 |
| B | 600 | 10 | 1.1 | 1077 | 19.5 | 2.8 | 400 | 93 | 5 | 51 | 16 | 7.0 | 0.3 | 3.2 | 1.0 | 3.3 |
| C | 500 | 10 | ~1 | 1075 | — | — | 325 | 94 | 7 | 58 | 19 | — | 2.0 | 4.6 | 1.3 | 3.5 |
| C | 500 | 10 | ~1 | 1075 | — | — | 325 | 91 | 9 | 58 | 17 | — | 1.3 | 3.8 | 0.7 | 5.3 |
| B. Stagnant deep-bed calcination (SDB) | | | | | | | | | | | | | | | | |
| A | 500 | 17 | 4.0 | 1083 | 16.3 | 14.0 | 350 | 95 | 21 | 70 | 5 | 1.2 | 0.4 | 3.7 | 0.22 | 17.0 |
| A | 650 | 17 | 4.0 | 1090 | 9.2 | 2.2 | 400 | 88 | 40 | 62 | 5 | 4.2 | 0.14 | 3.0 | 0.18 | 17.0 |
| C. Dry shallow-bed calcination (SBN) | | | | | | | | | | | | | | | | |
| B | 450 | 20 | 1.1 | 1061 | 17.2 | 0.1 | 375 | 91 | 12 | 44 | 28 | — | 0.53 | 4.6 | 2.0 | 2.3 |
| B | 500 | 10 | 1.1 | 1060 | 14.3 | 0.0 | 400 | 93 | 7 | 45 | 25 | — | 0.16 | 4.3 | 1.5 | 2.9 |
| B | 600 | 4 | 1.1 | 1074 | 3.6 | 0.0 | 400 | 75 | 9 | 29 | 34 | — | 0.04 | 4.8 | 6.5 | 0.7 |
| D. Shallow-bed steam calcination (SBST) | | | | | | | | | | | | | | | | |
| B | 400 | 4 | 1.1 | 1078 | 22.8 | 2.7 | — | — | — | — | — | 8.3 | — | — | — | — |
| B | 450 | 4 | 1.1 | 1078 | 22.0 | 2.2 | 375 | 95 | 6 | 59 | 7 | 9.9 | 0.36 | 0.23 | 2.3 | 0.3 |
| B | 500 | 4 | 1.1 | 1080 | 19.8 | 2.1 | 375 | 93 | 7 | 54 | 4 | 9.4 | 0.27 | 0.09 | 1.0 | 0.13 |

indicate DMA selectivity while values of $k_2/k_3 < 1$ indicate a product closer to the equilibrium value (*I*).

Space velocity, which correlates to catalyst activity, was obtained from the reactant feed rates and catalyst charge. Space velocity data at 90% MeOH conversion, 325°C, 1:1 NH₃ to MeOH feed composition, and 1 atm were used to compare catalyst activities. This basis demonstrates utility in the range of commercially practiced MeOH conversions and feed compositions at typical operating temperatures for H-ZK-5.

RESULTS

NH₄-ZK-5 Precursor

Unlike Cs,N_a-RHO, synthesis of Cs,K-ZK-5 does not result in large amounts of coexistent impurity phases. However, weak lines at $d = 11.2, 7.9, 6.4, 5.65,$ and 4.8 \AA were observed in the neutron diffraction pattern of a sample of ZK-5 that had been NH₄⁺ exchanged and calcined at 500°C in a stagnant deep-bed arrangement (7). These lines correspond approximately to a

hexagonal pattern that is indicative of an offretite-like phase with $a = 13.0$ and $c = 7.9 \text{ \AA}$. This seems reasonable in light of offretite formation in the nontemplated system $3\text{Na}_2\text{O} \cdot 0.5\text{K}_2\text{O} \cdot \text{Al}_2\text{O}_3 \cdot 10\text{SiO}_2$ (*10, 11*).

Effect of Calcination Temperature

Table 1 summarizes some physical properties and catalytic data obtained on H-ZK-5 samples prepared with high and low Cs content and calcined in DB, SDB, SBN, and SBST configurations. As with H-RHO, increasing calcination temperature (T_c) from 450 to 600°C under DB conditions increases DMA yields from 45 to 72% when ZK-5 contains ~4 Cs/uc. In addition, DME yields increase and activities decrease. However, at lower Cs levels (~1 Cs/cu), little change in DMA selectivity was observed for T_c between 450 and 500°C and DME yields are lower. Calcination at 600°C reduces DMA selectivities.

Increased dealumination and framework damage accompany increases in T_c as evidenced by IR, X-ray, and sorption data.

For example, increasing DB T_c from 450 to 600°C with 1.1 Cs/uc increases the framework stretching frequency, $\nu(\text{T-O})$, from 1071 to 1077 cm^{-1} . A rapid decrease in the intensity of the bridging OH bands at 3610 cm^{-1} was noted in H-ZK-5 DB-calcined above 500°C (7). Infrared data for H-ZK-5 with 3.9 Cs/uc do not show an increase in $\nu(\text{T-O})$ as T_c is increased (Table 1) although *n*-PrOH sorption decreases.

Methanol sorption measurements were used to estimate framework damage. Crystalline H-ZK-5 with 1.1 Cs/uc has a hypothetical methanol sorption capacity of 23.5 g/100 g based on the ZK-5 crystal structure and assuming that methanol packs as a liquid. Crystalline H-ZK-5 ($C_s = 1.1/\text{uc}$), DB-calcined at 400–500°C, has a methanol sorption capacity of ~ 20 g/100 g. The corresponding T-O stretching frequency is 1075 cm^{-1} . On the basis of the information in Table 1, samples calcined at 650°C in either SDB or SBN configuration are determined to have considerable framework damage.

Effect of Calcination Treatment

Although DB calcination results in highly DMA selective catalysts with both high and low C_s content, SBN calcination at $T_c = 450$ –500°C results in considerable framework damage as measured by lower DMA selectivity, and lower activities. At $T_c = 600$ °C the SBN sample, although showing $\nu(\text{T-O}) = 1074$ cm^{-1} , about equal to that of the DB sample, has undergone severe pore blockage that reduces MeOH sorption to 3.6% and SV to 0.04 h^{-1} . This contrasts with H-RHO where samples SBN-calcined over the range 400–700°C have high DMA selectivities (4).

It should also be noted that SBN calcination at 600°C leads to amorphitization of the zeolite whereas DB calcination at 600°C leads to a crystalline product (see Figs. 1 and 2). This may appear unusual but we have previously observed that amorphitization of H-RHO (4) and H-chabazite (5) oc-

TABLE 2
Infrared Data on ZK-5 Samples Calcined at 500°C

| Calcination | Main hydroxyl peak | | 3740 cm^{-1} height |
|-------------|--------------------|--------|------------------------------|
| | Position | Height | |
| SBN | 3610 | 2.5 | 0.3 |
| SBST | 3620 | 0.9 | 0.4 |
| SDB | 3640 | 0.9 | 0.5 |

cur at lower temperatures under SBN conditions than under DB conditions.

SDB calcination of ZK-5 with high C_s content produces highly DMA-selective catalysts although with high DME yields. The greatly reduced catalytic activity of a sample SDB-calcined at 650°C is accompanied by considerable framework damage ($\nu(\text{T-O}) = 1090$ cm^{-1} and lowered MeOH sorption (9.2%)).

The effect of SB calcination is particularly evident from X-ray diffraction patterns. Lower peak heights than those from DB calcination at similar T_c can be seen in Figs. 1 and 2; H-ZK-5 SB-calcined at 600°C is essentially amorphous as indicated from MeOH sorption of 3.6% and low space velocity of 0.04 h^{-1} . DB-calcined H-ZK-5 samples show strong 3740 cm^{-1} terminal OH bands (see Table 2), indicating considerable framework damage. Samples of H-ZK-5 listed in Table 2, although not identical to samples listed in Table 1, were typical of H-ZK-5 calcined under SBN, SBST, and SDB conditions.

SBN-calcined H-ZK-5 with 1.1 Cs/uc is slightly DMA-selective, showing $\sim 45\%$ DMA. The same samples SBST-calcined at either 400 or 500°C in steam (612 Torr) have higher DMA selectivity with 59% DMA and only a 6–7% DME yield. T-O stretching frequencies of SBST samples indicate substantially more framework dealumination than the SBN samples (1078 cm^{-1} for SBST vs ~ 1060 cm^{-1} for SBN). The X-ray diffraction patterns shown in Figs. 2 and 3 indicate that the SBST samples are more crystalline

than SBN samples. From Table 2 SBST samples show somewhat increased 3740 cm^{-1} terminal OH band development and decreased bridging OH content.

Reproducibility of ZK-5 Preparations

Catalytic properties of H-ZK-5 are apparently dependent on the purity of the synthesis product. SB-calcined sample B gave 65% DMA whereas sample C gave ~58% DMA. The lower selectivities of sample C may be a result of the debris noted in the SEM photos.

DISCUSSION

Comparison of H-ZK-5 with H-RHO

The ZK-5 framework is not as stable as the RHO framework. This is evidenced by shifts in $\nu(\text{T-O})$, loss of MeOH sorption capacity, and loss of X-ray crystallinity under calcination conditions which do not cause such changes in H-RHO. Catalytic and physical properties of ZK-5 similar to those of RHO are produced by calcination at temperatures ~100°C lower than those for RHO. Thus, maximum DMA selectivity is obtained for ZK-5 at $T_c = 450\text{--}500^\circ\text{C}$ whereas optimum DMA selectivity is obtained for RHO at $T_c = \sim 600^\circ\text{C}$ (4). Because the 3610 cm^{-1} OH band comes from the bridging OH in H-ZK-5 and H-RHO, reduction of the intensity of this band at higher calcination temperatures indicates framework damage. The maxima found in the intensity of the 3610 cm^{-1} bridging OH band at $T_c < 350^\circ\text{C}$ for H-ZK-5 and $T_c = 400^\circ\text{C}$ for H-RHO correlate with the optimum DMA selectivities found in H-ZK-5 and H-RHO. Similarly, maxima in the internal Lewis MeCN peak intensity were found at $T_c = 550$ and $>650^\circ\text{C}$, respectively, for H-ZK-5 and H-RHO.

In general the activity of H-ZK-5 is lower than that of H-RHO. Methylamine product selectivities that meet market demand are achieved with H-RHO at a median space velocity $\sim 3\text{ h}^{-1}$ at 325°C to give 90% MeOH conversion (4). Although fewer

H-ZK-5 samples were examined; it appears that product selectivities similar to those of H-RHO can be achieved at a median space velocity of $\sim 1\text{ h}^{-1}$. Thus, H-ZK-5 is about three times less active than H-RHO.

In zeolite H-RHO, high DMA selectivities were achieved without noticeable changes in the ratio of methanol to *n*-propanol sorption which remained low as T_c and DMA selectivity increased. In H-ZK-5, however, as T_c is increased, DMA selectivities and GSI increase concomitantly. However, an elevated GSI is clearly not necessary to obtain good DMA selectivity; one sample, SDB-calcined at 500°C , exhibited a GSI of only 1.2 but provided a DMA selectivity of 70%.

DMA selectivities of SBST-calcined ZK-5 compare well with those of SBST-calcined H-RHO. The DMA selectivities of SBST-calcined H-RHO are somewhat higher than those of SBST-calcined H-ZK-5 but the synthesis parameters were not optimized for H-ZK-5.

As noted earlier, SBST-calcined H-ZK-5 shows more framework dealumination than SBN H-ZK-5, as evidenced by $\nu(\text{T-O}) = 1080\text{ cm}^{-1}$ and a strong 3740 cm^{-1} terminal OH band. Although these strong OH bands have been associated with framework damage, this is not consistent with the unusually sharp and strong diffraction peaks in Fig. 3. The X-ray pattern may reflect a highly crystalline framework whereas the IR bands at 3740 cm^{-1} may indicate non-crystalline regions, perhaps isolated in mesopores as proposed by Lohse and Mildebrath (12) for ultrastable Y.

Cs content plays an important role in determining the catalytic properties of H-ZK-5. Most DB-calcined samples with ~ 1 Cs/uc have significantly higher DMA selectivities than similarly calcined samples with ~ 4 Cs/uc. The exceptions to this rule have high DME yields (20–40%). This may not be a good comparison because of the different zeolite bases. However, in light of the similar DMA selectivity obtained with sam-

ple B vs sample C (65% vs 58%, respectively), we believe this dependency of DMA selectivities upon Cs content to be real. DME yields also correlate with Cs content. The samples containing 4 Cs/uc (sample A, DB-calcined and SDB-calcined) both produce more DME (15–40%) than samples B and C with ~1 Cs/uc.

SUMMARY

Selectivity and activity of zeolite H-ZK-5 in the synthesis of dimethylamine from methanol and ammonia are dependent upon the Cs content of the NH₄-ZK-5 precursor and the temperature and atmosphere of calcination. The most active and highly DMA-selective catalysts result from deep-bed calcination of NH₄-ZK-5 containing ~1 Cs/uc. By comparison increased Cs content seems to result in higher DMA yield. Steaming under shallow-bed or deep-bed conditions results in high DMA selectivities but lower activities, whereas shallow-bed dry calcination results in significantly lower DMA selectivities, presumably because of pore blockage and amorphitization.

By comparison with zeolite H-RHO, zeolite H-ZK-5 is less thermally stable and has lower activity in DMA synthesis from methanol and ammonia.

ACKNOWLEDGMENTS

We thank M. VanKavelaar for scanning electron micrographs and R. Harlow for assistance in obtaining X-ray diffraction data.

REFERENCES

1. Keane, W., Sonnichsen, G. C., Abrams, L., Corbin, D. R., Gier, T. E., and Shannon, R. D., *Appl. Catal.* **32**, 361 (1987).
2. Gier, T. E., Shannon, R. D., and Sonnichsen, G. C., U.S. Patent 4,602,112 (July 22, 1986).
3. Abrams, L., Gier, T. E., Shannon, R. D., and Sonnichsen, G. C., Eur. Patent Applic. 183,423 (April 6, 1986).
4. Shannon, R. D., Keane, M., Abrams, L., Staley, R. H., Gier, T. E., Corbin, D. R., and Sonnichsen, G. C., *J. Catal.* **113**, 367 (1988).
5. Shannon, R. D., Keane, M., Abrams, L., Staley, R. H., Gier, T. E., Corbin, D. R., and Sonnichsen, G. C., *J. Catal.* **114**, 8 (1988).
6. Robson, H. E., U.S. Patent 3,720,753 (March 13, 1973).
7. Fischer, R. X., Baur, W. H., Shannon, R. D., Staley, R. H., Vega, A. J., Abrams, L., and Prince, D., *Zeolites* **6**, 378 (1986).
8. Fischer, R. X., Baur, W. H., Shannon, R. D., Staley, R. H., Vega, A. J., Abrams, L., and Prince, E., *J. Phys. Chem.* **90**, 4414 (1986).
9. Shannon, R. D., Staley, R. H., and Auroux, A., *Zeolites* **7**, 301 (1987).
10. Gier, T. E., unpublished data.
11. Sand, L. B., U.S. Patent 4,093,699 (June 6, 1978).
12. Lohse, U., and Mildebrath, M., *Z. Anorg. Allg. Chem.* **476**, 126 (1981).